

**A wash-free fluorescent probe with a large Stokes shift for the identification of  
NAFL through tracing the change of lipid droplets**

Jing Yang<sup>a,b</sup>, Zhiyu Wang<sup>a,b</sup>, Yi Deng<sup>a,b</sup>, Cuifeng Zhang<sup>c</sup>, Xuebin Shen<sup>a,b</sup>, Jing He<sup>d</sup>, Lei  
Hu<sup>a,b,\*</sup>, Hui Wang<sup>a,b,\*</sup>

[a] *Anhui Innovative Center for Drug Basic Research of Metabolic Diseases, Wannan Medical  
College, Wuhu 241002, China*

[b] *School of Pharmacy, Wannan Medical College, Wuhu 241002, China*

[c] *School of Anesthesiology, Wannan Medical College, Wuhu 241002, China*

[d] *Department of Medical Biology, Wannan Medical College, Wuhu 241002, China*

\* Corresponding author

*E-mail address:* hulei@wnmc.edu.cn (Lei Hu); [wanghias@126.com](mailto:wanghias@126.com) (Hui Wang)

## **Experimental section**

### **Measurements and apparatus**

All chemicals and solvents were used without further purified. <sup>1</sup>H-NMR spectra were measured on a Bruker Advance 400 spectrometer. HRMS spectra were measured on Agilent 7250& JEOL-JMS-T100LP AccuTOF. UV-*vis* absorption spectra were measured on UV-5900 spectrophotometer. Fluorescence spectra were measured on HITACHI F-4600 fluorescence spectrophotometer (Measurement of parameters:  $\lambda_{\text{ex}}$ =500 nm; spectral slit width=10 nm; voltage=500 V). Cell imaging was imaged on a Leica TCS SP8 confocal laser scanning microscope. Image data acquisition and processing were performed using Image J.

### **Computational details**

Optimizations were carried out with B3LYP without any symmetry restraints, and the TD-DFT [B3LYP] calculations were performed on the optimized structure. All calculations were performed with the G09 software. Geometry optimization of the singlet ground state and the TD-DFT calculation of the lowest 25 singlet-singlet excitation energies were calculated with a basis set composed of 6-31G\* for all atoms

were download from the EMSL basis set library.

### **Cytotoxicity assays**

HepG2 cells were prepared for cell viability studies in 96-well plates at a density of  $10^4$  cells/well. Cells were grown to ~85% confluence in 96-well plates before treatment. Probes **LD-HWZ** was then added at indicted concentrations to triplicate wells. Prior to the compound' treatment, cell culture medium was changed, and aliquots of the compounds stock solutions were diluted to obtain the final concentrations. After incubation for 24 h, the medium was replaced with fresh DMEM medium. Subsequently, cells were treated with 5 mg/mL MTT (10  $\mu$ L/well) and incubated for an additional 4 h (37 °C, 5% CO<sub>2</sub>). After MTT medium removal, the formazan crystals were dissolved in DMSO (100  $\mu$ L/well) and the absorbance was measured at 590 nm using a microplate reader (Infinite 2000pro).

### **Confocal fluorescence imaging**

HepG2 cells were seeded in 35 mm glass bottom plates at a density of  $1 \times 10^5$  cells, and cells were grown to 60~65% confluence in per plates before treatment. Probe **LD-HWZ** was first dissolved in DMSO to 1 mM as stock solution, and then diluted by DMEM cell culture medium to the working concentration (10  $\mu$ M). For live cell imaging, cells were incubated with probe **LD-HWZ** at 10  $\mu$ M in cell medium containing 10 % FBS and maintained at 37 °C in an atmosphere of 5% CO<sub>2</sub> and 95% air for 30 min, respectively. The cells were then washed with or without PBS buffer before imaging.

### **Co-localization experiments**

Co-staining was performed using 1  $\mu$ M BODIPY 493/503 and Lyso-tracker Red, respectively for 30 min. For BODIPY,  $\lambda_{ex}$  = 488 nm;  $\lambda_{em}$  = 500-550 nm. For Lyso-tracker,  $\lambda_{ex}$  = 561 nm;  $\lambda_{em}$  = 580-620 nm.

### **LDs production experiments induced by Oleic Acid.**

HepG2 cells were seed on glass-bottomed confocal dishes for 24 h, and then were treated with different concentrations of oleic acid for 6 h, respectively, while the cells were treated with oleic acid (100  $\mu$ M) for 0, 2, 4 and 6 h, respectively. Each experiment was performed for three independent times.

### **Animal model and tissues imaging**

All animal experiments were conducted according to the Guidance for Ethical Treatment of Laboratory Animals, and the experimental protocols were approved by the Institutional Animal Care and Use Committee at the Wannan Medical College (Anhui, China) (No. WNMC-AWE-2023258). We have exerted ourselves to reduce the number of animals used in these studies and also taken effort to reduce animal suffering from pain and discomfort. The fatty liver mice model was constructed by feeding the C57 mice (six-week-old, male) on a 60% high fat diet with choline deficiency feed for 2 months. Meanwhile, the control mice were prepared by feeding normal forage. Mice were anaesthetized and sacrificed, and the liver organ (including normal liver and fatty liver) was carefully isolated. A fraction of the liver organs (including normal liver and fatty liver) were sectioned by frozen to 10  $\mu$ m thicknesses for tissue imaging. Prior to imaging, the slices were stained with **LD-HWZ** (10  $\mu$ M) for 30 min at 37 °C. Tissue imaging were obtained by Leica TCS SP8. The hematoxylin and eosin (HE) and Oil Red O experiments were obtained on Olympus BX53.

### **Synthesis of probe LD-HWZ**

To a 100 mL round-bottomed flask, 2-(3,5,5-trimethylcyclohex-2-en-1-ylidene)malononitrile (0.19 g, 1 mmol) was added and dissolved in 20 mL ethanol. Then 4-(diphenylamino)-2-hydroxybenzaldehyde (0.29 g, 1 mmol), 50  $\mu$ L piperidine were added, and the mixture was refluxed for about 24 h. After the reaction finished, the mixture was cooled to room temperature. The ethanol was vacuum dried in a rotatory evaporator and the crude product was purified by silica gel column chromatography (petroleum ether: ethyl acetate=5:1, V/V) to obtain a black solid (0.12 g). Yield: 26%.  $^1\text{H}$  NMR (400 MHz,  $d_6$ -DMSO)  $\delta$  10.06 (s, 1H), 7.34-7.36 (m, 5H),

7.23-7.11 (m, 7H), 6.92 (d,  $J = 7.6$  Hz, 1H), 6.76 (s, 1H), 6.47 (s, 1H), 6.35 (d,  $J = 8.4$  Hz, 1H), 2.51 (s, 4H), 1.01 (s, 6H). HRMS: Calculated: 457.2154; Found: 458.2248 ( $[M+1]^+$ ).  $^{13}\text{C}$  NMR (101 MHz,  $\text{CDCl}_3$ )  $\delta$  169.45, 155.70, 150.60, 146.59, 132.31, 129.51, 128.66, 126.88, 125.81, 124.36, 122.09, 116.67, 114.45, 114.09, 113.28, 43.09, 39.14, 32.02, 28.04.

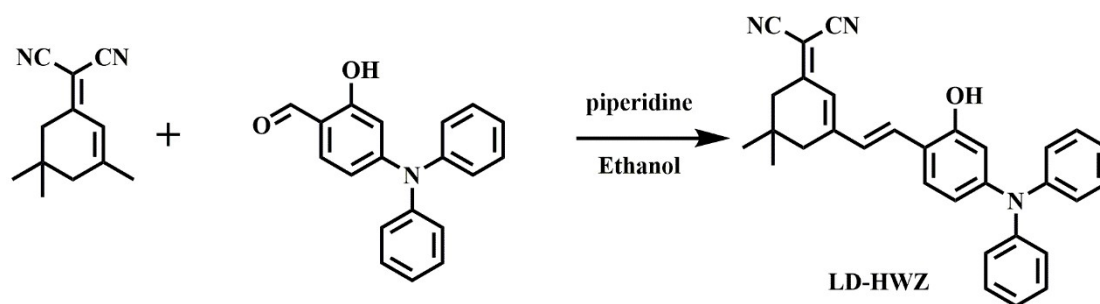


**Fig S1** The synthetic route of LD-HWZ.

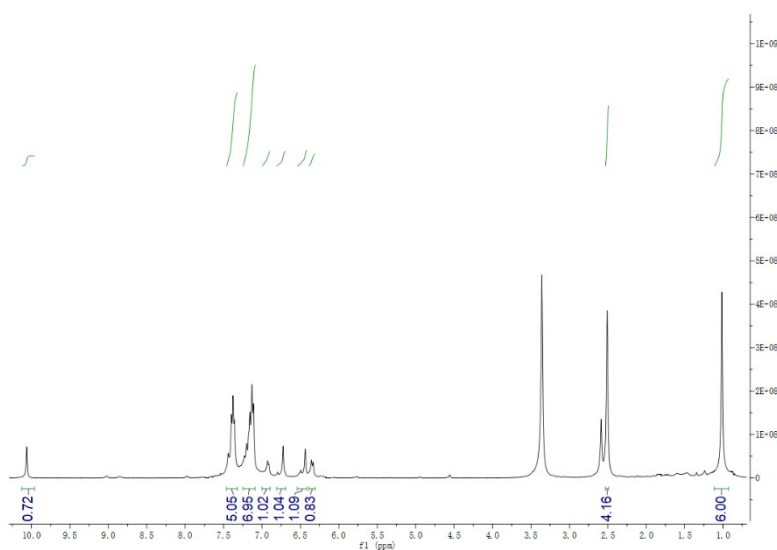


**Fig S2**  $^1\text{H}$  NMR of LD-HWZ.

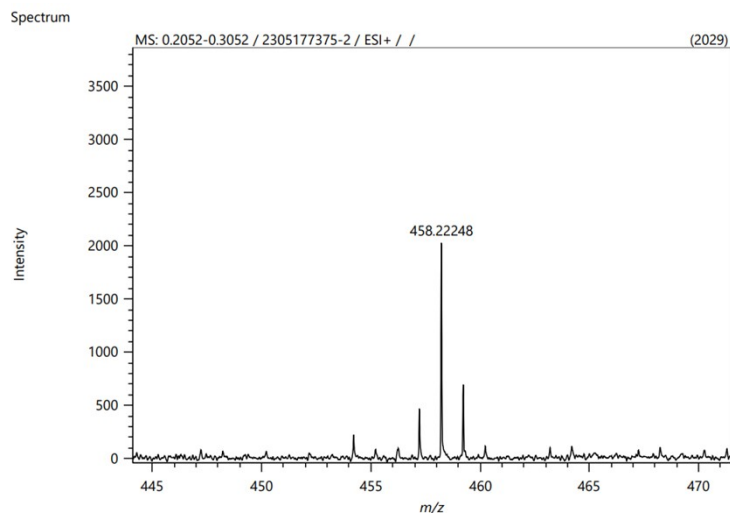


**Fig S3** HRMS of probe **LD-HWZ**.

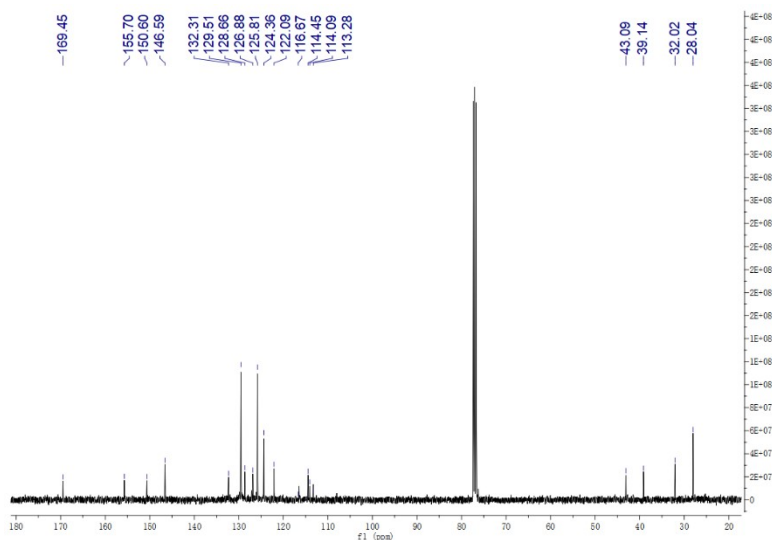


**Fig S4**  $^{13}\text{C}$  NMR of probe **LD-HWZ**.

**Table S1** The optical properties of probe **LD-HWZ**.

$\square$	DOA	THF	EA	EtOH	ACN	DMSO	PBS
$\lambda_{\text{abs, max}}/\text{nm}$	484	503	497	508	494	518	520
$\lambda_{\text{em, max}}/\text{nm}$	615	637	632	666	668	679	697
Stokes shift/nm	131	134	135	158	174	161	177
$\epsilon/L \cdot \text{mol}^{-1} \cdot \text{cm}^{-1}$	23260	44400	43850	43340	44420	41900	18390
QY <sup>[a]</sup> /%	2.01	1.23	1.07	3.65	1.72	2.42	0.05

[a] Quantum yields determined by using Rhodamine B as standard.

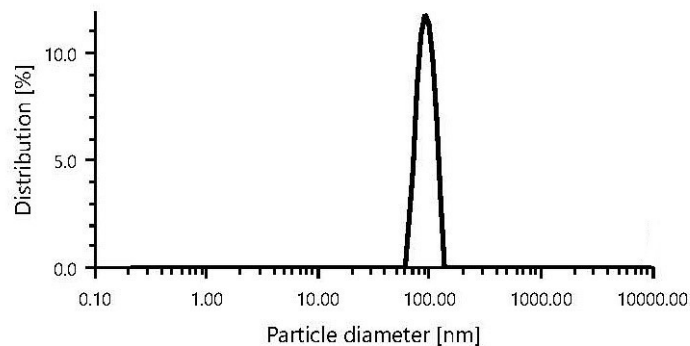


**Fig S5** The particle size distribution of **LD-HWZ** (10 μM) in PBS buffer by DLS.

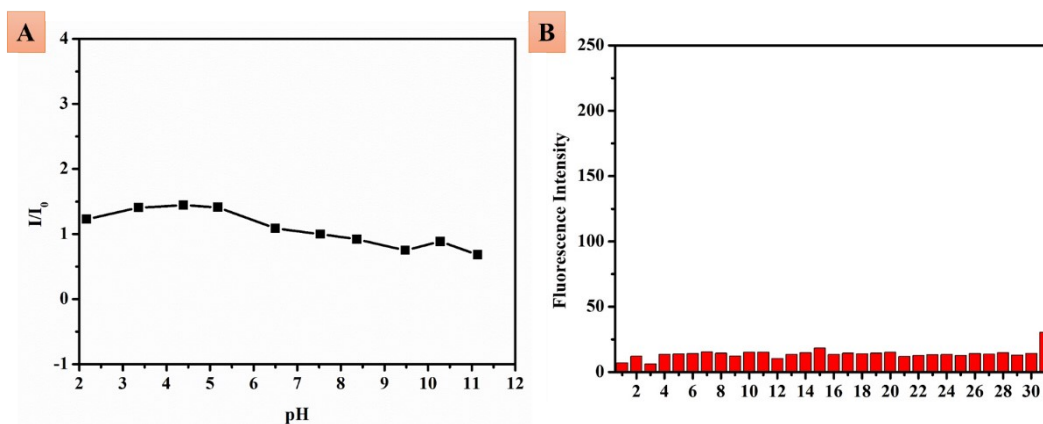


**Fig S6** (A) Fluorescence intensity ratios of **LD-HWZ** in different pH buffers; (B) Variation of emission intensity in the presence of various species. 1, PBS; 2,  $\text{Ca}^{2+}$ ; 3,  $\text{Cu}^{2+}$ ; 4, Cys; 5, GSH; 6,  $\text{H}_2\text{O}_2$ ; 7, Hcy; 8,  $\text{Cl}^-$ ; 9, L-Alanine; 10, L- Phenylalanine ; 11, L- Glutamic acid; 12, L- Arginine; 13, L- Lysine; 14, L- Proline; 15, L- Tryptophan; 16, L- Serine; 17, L- Threonine; 18, L- Valine; 19, L-Isoleucine; 20, L- Histidine; 21,  $\text{Mg}^{2+}$ ; 22,  $\text{HPO}_4^{2-}$ ; 23,  $\text{S}_2\text{O}_5^{2-}$ ; 24,  $\text{SO}_4^{2-}$ ; 25,  $\text{F}^-$ ; 26,  $\text{HSO}_3^-$ ; 27,  $\text{NO}_2^-$ ; 28,  $\text{NO}_3^-$ ; 29, VC; 30, Glucose; 31, BSA.

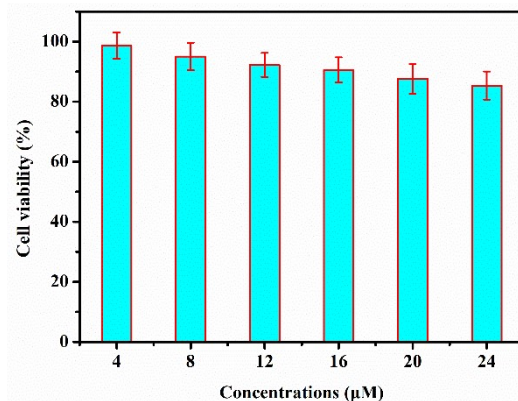


**Fig S7** Cell viability of **LD-HWZ** on HepG2 cells by MTT assay.

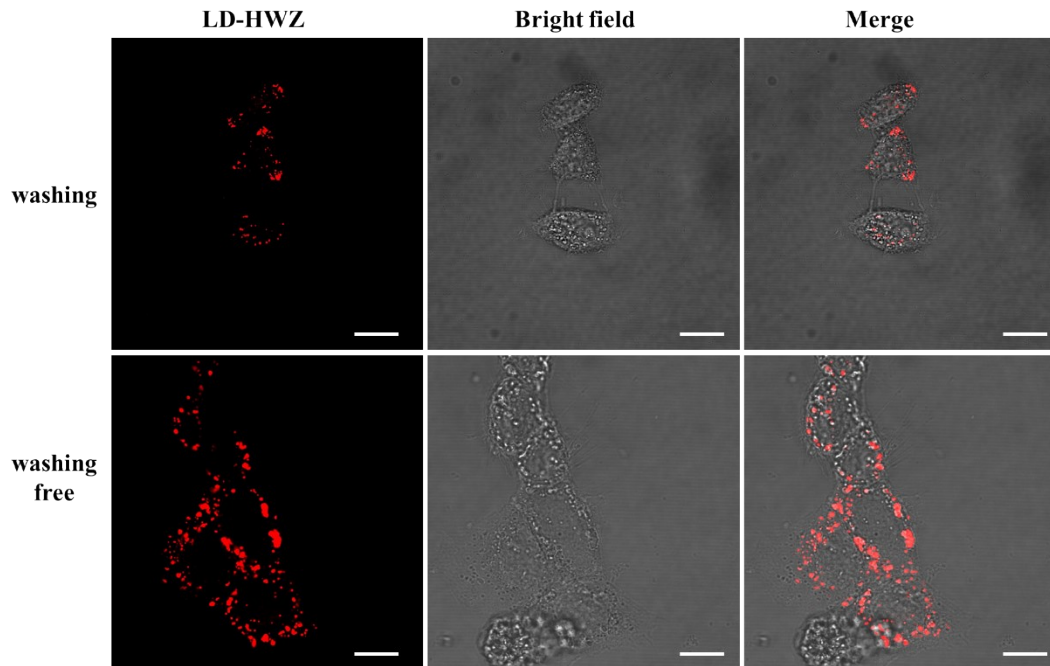


**Fig S8** Confocal microscopy images of **LD-HWZ** (10  $\mu$ M) through wash or wash-free procedure. Scale bar: 10  $\mu$ m.

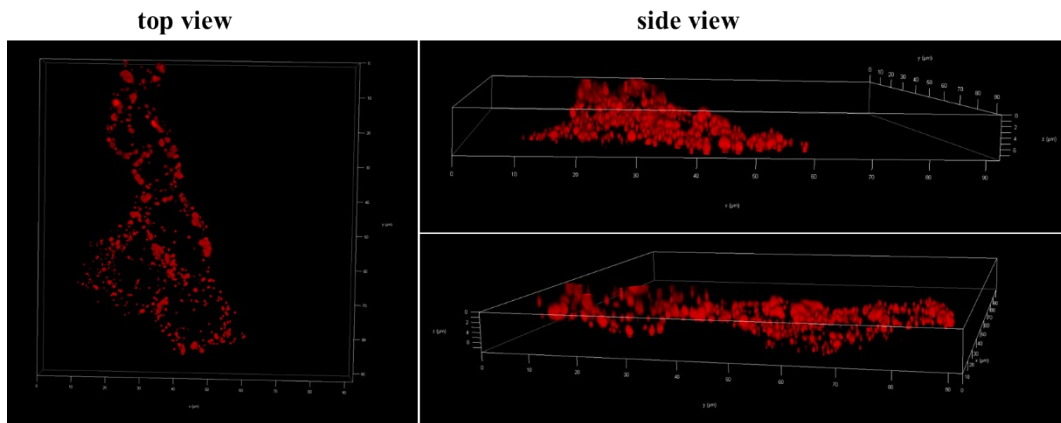


**Fig S9** 3D imaging of lipid droplets in HepG2 cells with **LD-HWZ** (10  $\mu$ M).

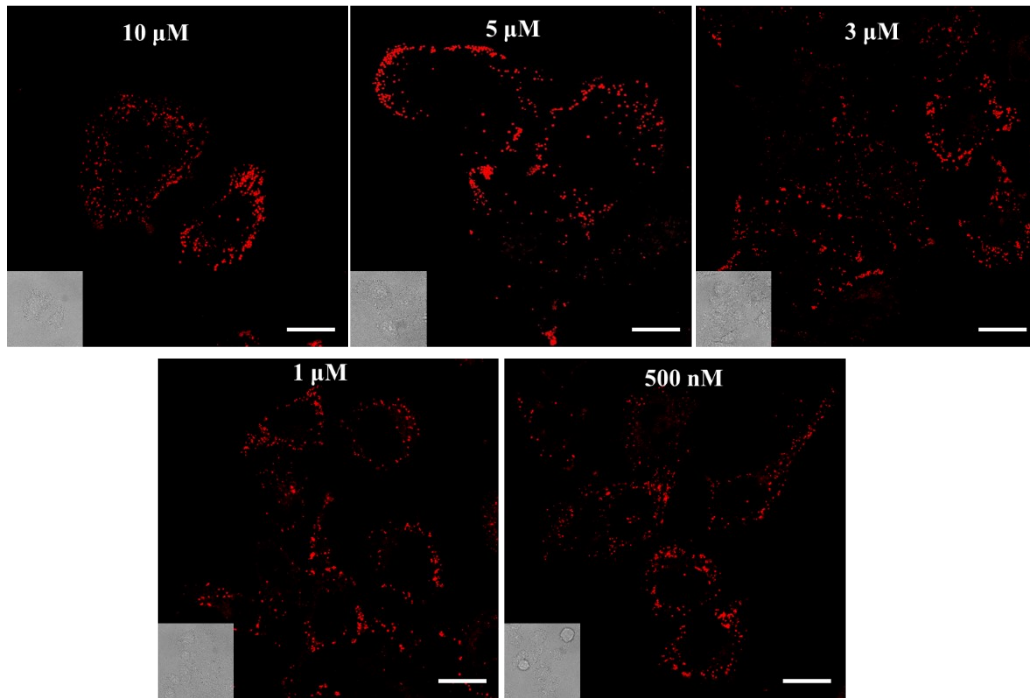


**Fig S10** Confocal laser imaging of HepG2 cells stained with different concentrations of LD-HWZ. Scale bar: 10  $\mu\text{m}$ .

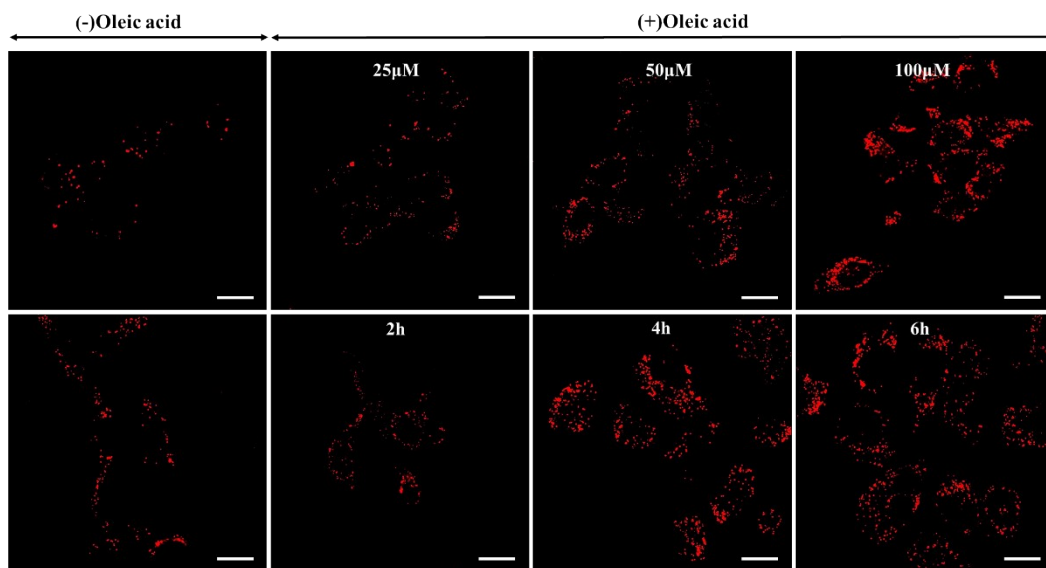


**Fig S11** Fluorescence images of HepG2 cells incubated with oleic acid under different conditions of concentration and time, followed by staining with LD-HWZ (10  $\mu\text{M}$ ). Scale bar: 20  $\mu\text{m}$ .

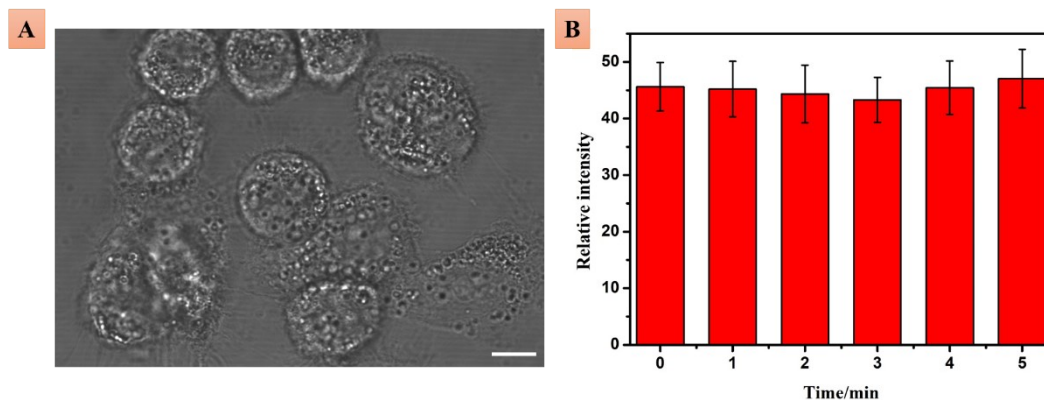


**Fig S12** (A) Bright field images of HepG2 cells. Bar: 10 μm; (B) The histograms of the fluorescence intensity of probe **LD-HWZ** incubated with HepG2 cells at different time.

Table R2 The comparison with the performance of known LDs-fluorescent probes.

Probe	emission wavelength	The lowest concentration to enter the cell	Operating procedure	Application	Ref
TPA-LD	630 nm	10 μM	washing	cell and zebrafish imaging	1
NICSF-T	445 nm	10 μM	washing	cell imaging	2
DBC30	< 500 nm	1 μM	washing	cell and tissues imaging	3
TPA-CYP	690 nm	15 μM	washing	cell imaging, zebrafish imaging	4
LIP-Ser	722 nm	10 μM	washing	cell imaging, tissues imaging	5
TPE-BET	520 nm	5 μM	washing	cell imaging	6
2h	164 nm	10 μM	washing	cell and zebrafish imaging	7
TP-LDs	650 nm	1 μM	washing	cell, organs and tissues imaging	8

DPBT	650 nm	/	washing	cell and tissues imaging	9
TITM	600 nm	1 $\mu$ M	washing	cell and tissues imaging	10
MeO- TTM	600 nm	10 $\mu$ M	washing	cell and tissues imaging	11
LD-HWZ	697 nm	500 nM	washing-free	cell imaging, tissues imaging	this work

#### References:

- [1] X. Zhang, L. Yuan, J. X. Jiang, J. W. Hu, A. D. Rietz, H. Z. Cao, R. L. Zhang, X. H. Tian, F. L. Zhang, Y. G. Ma, Z. P. Zhang, K. Uvdal, Z. J. Hu. *Anal. Chem.*, 2020, 92, 3613-3619.
- [2] Q. S. Shi, Y. Y. Ni, L. M. Yang, L. Kong, P. Y. Gu, C. Y. Wang, Q. C. Zhang, H. P. Zhou and J. X. Yang, *J. Mater. Chem. B*, 2023, 11, 6859-6867.
- [3] K. Purevsuren, Y. Shibuta, S. Shiozaki, M. Tsunoda, K. Mizukami, S. Tobita, T. Yoshihara. *J. Photoch. Photobio. A*, 2023, 438, 114562.
- [4] S. Z. Pei, H. Y. Li, J. L. Li, Y. Liu, G. M. Zhang, L. H. Shi, W. T. Liang, C. H. Zhang, S. M. Shuang and C. Dong, *ACS Biomater. Sci. Eng.*, 2023, 9, 3590-3596.
- [5] W. B. Wang, L. Chai, X. Chen, Z. Y. Li, L. Y. Feng, W. Hu, H. B. Li and G. f. Yang, *Biosens. Bioelectron.*, 2023, 231, 115289.
- [6] B. Lin, Z. R. Li, Y. N. Lin, Y. Shu and J. H. Wang, *Anal. Chim. Acta*, 2023, 1279, 341776.
- [7] W. L. Cui, M. H. Wang, Y. H. Yang, J. Y. Wang. *Org. Biomol. Chem.*, 2023, 21, 2960-2967.
- [8] Y. Y. Pu, R. D. Huang, L. Chai, H. H. Yang, D. N. Wang, Z. L. Wei, Z. X. Zhan. *Sens. Actuators B Chem.*, 2023, 380, 133343.

- [9] Z. Zheng, Y. C. Yang, P. P. Wang, X. X. Gou, J. Y. Gong, X. Q. Wu, Z. W. Bao, L. J. Liu, J. Zhang, H. Zou, L. Zheng, B. Z. Tang. *Adv. Funct. Mater.*, 2023, 33. 2303627.
- [10] C. M. Li, W. H. Zhuang, Y. C. Wang, S. F. Li, J. R. Chen, L. S. Zhou, Y. B. Liao, M. Chen, Y. S. You. *Dyes Pigm.*, 2022, 204, 110439.
- [11] Y. Zhang, W. H. Zhuang, J. R. Chen, C. M. Li, S. F. Li, M. Chen. *Spectrochim. Acta A*, 2023, 286, 122017.